2011 50th IEEE Conference on Decision and Control and
European Control Conference (CDC-ECC)
Orlando, FL, USA, December 12-15, 2011

PD+ Based Spacecraft Attitude Tracking with Magnetometer Rate Feedback

Raymond Kristiansen, Rune Schlanbusch and Espen Oland

Abstract— **In this paper we present a solution to spacecraft attitude tracking control utilizing a passivity-based PD+ control solution with magnetometer rate feedback. This solution aims toward small spacecraft with size and weight constraints, which typically carries *e.g.* solar sensors and magnetometers for attitude determination, but no sensors for angular velocity feedback. The result is a control solution which uses magnetometer rate feedback to provide angular velocity information, while at the same time exploits the natural passivity in the system. The equilibrium points in the resulting closed-loop system are proved to be uniformly asymptotically stable under some mild gain conditions, and controller performance is visualized through simulations.**

I. INTRODUCTION

Electromagnetic actuation has proven to be a valid approach for spacecraft attitude control in Earth orbits, and in particular for small spacecraft with hard requirements on available mass and weight. The concept is based on the fact that the Earth is surrounded by a time-varying magnetic field, and by inducing local magnetic field vectors around spacecraft axes the natural push-pull motion resulting from interfering magnetic field may be used to create torques for spacecraft attitude maneuvers [1]. The dawn of attitude stabilization using electromagnetic actuation may, according to the thorough review in [2] be traced back to the early sixties; however, the first attempted approximate solution to the problem was presented in [3]. Then, after some dormant years, the problem spawned significant interest from late eighties with the combined electromagnetic and gravity gradient stabilization solutions given in [4]–[8], as well as control solutions by means of electromagnetic actuation only –*cf.* [9]. Most of these results incorporate assumptions of periodicity in the magnetic field and state feedback of spacecraft attitude to achieve local asymptotic stability properties. Other solutions have also been proposed based on measurements of magnetic field vectors, such as [10]–[13], which utilize a combination of the field vectors and their rate. These solutions are attractive in their own respect, and enable a spacecraft to achieve stabilization with magnetometers and magnetic actuators as onboard determination and control hardware; however, they are bound to the properties of the magnetic field, and represent therefore control solutions which do not adhere to the natural motion of the spacecraft. Solutions which incorporate the natural motion of spacecraft are typically those which aim to preserve passivity properties, such as [14]–[17]. In addition, several solutions have been proposed to the problem of spacecraft attitude control without angular velocity measurements; one approach is to use model-based nonlinear observers to estimate the angular velocity, as suggested in *e.g.* [18], [19]. Other solutions, such as in [20]–[25] employ variations of first-order filters that, if not supplying the controller with the correct angular velocity, at least provides enough information to solve the control problem. For small spacecraft with limited computational resources, this approach may be favorable.

However, a better solution would be to design an output feedback controller using the vectorial measurements from the sensors directly without the need for state estimation, while at the same time preserving the natural passivity in the system. In this paper, we introduce a passivity-based control solution for spacecraft attitude tracking using attitude quaternion and magnetometer rate feedback. This solution aims to combine the natural passivity with the use of lightweight magnetometer sensors to achieve damping, and is suitable for small spacecraft equipped with magnetometers and solar sensors for attitude determination. Roughly speaking, the main idea is to combine the well known passivity-based PD+ controller from [26] which has proven successful in the control of Euler-Lagrange systems (*cf.* [27]), with the classical b-dot control law in [3] typically used for spacecraft detumbling operations. This solution may be considered as a first step towards passivity-based output feedback magnetic control; however, to maintain focus on the main contribution of introducing magnetometer rate feedback in the loop, we have chosen to present the main result with general 3DOF actuation, which may be provided by means of *e.g.* reaction wheels or thruster systems. As a starting point for incorporating actuators, the reader is referred to [28], where results on actuator combinations are presented and analyzed using passivity.

II. PRELIMINARIES

We denote by $\|\cdot\|$ the Euclidean norm of a vector and the induced $\mathcal{L}_2$ norm of a matrix. Reference coordinate frames are denoted by $\mathcal{F}^{(\cdot)}$, and in particular we use the standard definition of the Earth-Centred Inertial (ECI) frame $\mathcal{F}^i$, with z axis towards celestial north, normal to the equatorial plane. Moreover, we define a body frame $\mathcal{F}^b$, with origin in the spacecraft center of mass and axes fixed to the spacecraft body. We denote by $\boldsymbol{\omega}_{b,a}^c$ the angular velocity of $\mathcal{F}^a$ relative to $\mathcal{F}^b$, referenced in $\mathcal{F}^c$. Matrices representing coordinate transformation from $\mathcal{F}^a$ to $\mathcal{F}^b$ are denoted $\mathbf{R}_a^b$. We denote by $\mathbf{S}(\cdot) \in \left\{\mathbf{S}(\cdot) \in \mathbb{R}^{3\times 3} : \mathbf{S}(\cdot) + \mathbf{S}^\top(\cdot) = \mathbf{0}\right\}$ the cross product operator, such that for arbitrary vectors $\mathbf{v}_1 \in \mathbb{R}^3$ and

R. Kristiansen, R. Schlanbusch and E. Oland are with the Department of Technology, Narvik University College, N-8505 Narvik, Norway {rayk, runsch, eol}@hin.no

$\mathbf{v}_2 \in \mathbb{R}^3$ we have $\mathbf{S}(\mathbf{v}_1)\mathbf{v}_2 = \mathbf{v}_1 \times \mathbf{v}_2$. Hence, we also have that $\mathbf{S}(\mathbf{v}_1)\mathbf{v}_2 = -\mathbf{S}(\mathbf{v}_2)\mathbf{v}_1$. When the context is sufficiently explicit, we may omit to write arguments of functions.

III. SYSTEM MODEL

A. Body frame rotation

Rotations are typically represented by rotation matrices belonging to $SO(3) = \{\mathbf{R} \in \mathbb{R}^{3\times 3} : \mathbf{R}^\top\mathbf{R} = \mathbf{I}, \det\mathbf{R} = 1\}$. In particular, the rotation matrix describing rotations from the body frame $\mathcal{F}^b$ to the inertial frame $\mathcal{F}^i$ can be described by

$$\mathbf{R}_b^i = \mathbf{I}+2\eta\mathbf{S}(\boldsymbol{\epsilon}) + 2\mathbf{S}^2(\boldsymbol{\epsilon}) \tag{1}$$

where $\mathbf{q} = \left[\eta,\ \boldsymbol{\epsilon}^\top\right]^\top$ is a unit quaternion, which satisfy the constraint

$$\eta^2 + \boldsymbol{\epsilon}^\top\boldsymbol{\epsilon} = 1\,. \tag{2}$$

The set of unit quaternions is a non-commutative multiplicative group denoted $S^3 = \{\mathbf{q} \in \mathbb{R}^4 : \|\mathbf{q}\| = 1\}$. The group is a covering manifold of $SO(3)$, and provides a globally nonsingular parametrization of the latter. The inverse rotation is given by the inverse unit quaternion $\mathbf{q}^{-1} = \left[\eta,\ -\boldsymbol{\epsilon}^\top\right]^\top$, and the quaternion product is defined as (*cf.* [29])

$$\mathbf{q}_1 \otimes \mathbf{q}_2 := \begin{bmatrix} \eta_1\eta_2 - \boldsymbol{\epsilon}_1^\top\boldsymbol{\epsilon}_2 \\ \eta_1\boldsymbol{\epsilon}_2 + \eta_2\boldsymbol{\epsilon}_1 + \mathbf{S}(\boldsymbol{\epsilon}_1)\boldsymbol{\epsilon}_2 \end{bmatrix}. \tag{3}$$

Finally, we note that a unit quaternion with the scalar parameter $\eta > 0$ satisfies the property

$$0 \leq (1-\eta)^2 \leq (1-\eta)(1+\eta) = 1-\eta^2 = \boldsymbol{\epsilon}^\top\boldsymbol{\epsilon}\,. \tag{4}$$

B. Rotational Motion

The attitude kinematics can be expressed as

$$\dot{\mathbf{q}} = \mathbf{T}(\mathbf{q})\boldsymbol{\omega}, \quad \mathbf{T}(\mathbf{q}) = \frac{1}{2}\begin{bmatrix} -\boldsymbol{\epsilon}^\top \\ \eta\mathbf{I} + \mathbf{S}(\boldsymbol{\epsilon}) \end{bmatrix} \tag{5}$$

where we denote for simplicity $\boldsymbol{\omega} = \boldsymbol{\omega}_{i,b}^b$. Moreover, the attitude dynamics can be expressed as

$$\mathbf{J}\dot{\boldsymbol{\omega}} = \boldsymbol{\tau} - \mathbf{S}(\boldsymbol{\omega})\mathbf{J}\boldsymbol{\omega} \tag{6}$$

where $\mathbf{J} = \mathbf{J}^\top > \mathbf{0}$ is the spacecraft inertia matrix which satisfies $j_m \leq \|\mathbf{J}\| \leq j_M$ with $j_M \geq j_m > 0$, and $\boldsymbol{\tau}$ denotes external and internal torques working on the spacecraft body. In general, the torque may be expressed as $\boldsymbol{\tau} = \boldsymbol{\tau}_a + \boldsymbol{\tau}_d$, where $\boldsymbol{\tau}_a$ and $\boldsymbol{\tau}_d$ denotes actuator torques and disturbance torques respectively, but for simplicity we assume here that $\boldsymbol{\tau}_d = \mathbf{0}$. Hence, the total system given by (5)-(6) evolves on the manifold $\mathcal{M} = S^3 \times \mathbb{R}^3$.

C. Magnetic Determination and Control

Magnetic determination and control involves the use of magnetometers for sensing of the surrounding geomagnetic field of the Earth, as well as magnetic torquers for producing a magnetic moment which provides torque when interacting with the geomagnetic field. To determine the spacecraft attitude, a minimum of two vector measurements are necessary, and a combination of solar sensors and magnetometers is a popular choice. By working these sensors in combination, one may employ *e.g.* a TRIAD algorithm to estimate the attitude during operational phases –*cf.* [30].

1) Geomagnetic Field: Under the assumptions that only negligible electric field changes occur and that the amount of current flowing across the boundary between the Earth and the atmosphere is relatively significant, a solution for the main geomagnetic field of the earth can according to [31] be obtained from the negative gradient of a scalar potential as

$$\mathbf{b} = -\left[\mathbf{i}\frac{\partial U}{\partial x} + \mathbf{j}\frac{\partial U}{\partial y} + \mathbf{k}\frac{\partial U}{\partial z}\right] = -\nabla U \tag{7}$$

where $\mathbf{i}, \mathbf{j}$ and $\mathbf{k}$ represents three orthogonal directions. When the assumption is made that essentially all contributions to the field comes from the internal Earth sources, the scalar potential can be expressed in spherical coordinates as

$$U(r,\theta,\phi) = R_e \sum_{n=1}^{\infty}\left[\left(\frac{R_e}{r}\right)^{n+1} F_n^i(\phi,\theta)\right] \tag{8}$$

where θ and ϕ are the geographic, Earth-centered coordinates of the radial distance, *co-latitude* and longitude, respectively, $R_e = 6371.2$ km is the Earth radius, r is the orbit radius and $F_n^i(\phi,\theta)$ is the *Legendre polynomial* of the independent variable θ that is multiplied by sine and cosine of the independent variable ϕ. The labeling superscript i indicates internal source terms of the potential functions. The Legendre polynomial $F_n^i(\phi,\theta)$ can be expressed as

$$F_n^i(\phi,\theta) = \sum_{m=0}^{n}\left[g_n^m\cos(m\phi) + h_n^m\sin(m\phi)\right]P_n^m(\theta)$$

where g_n^m and h_n^m are Gaussian coefficients, and $P_n^m(\theta)$ is the Gauss function of co-latitude only. Note that $n \geq 1$ and $n \geq m \geq 0$. With a degree $n = 1$ and order $m = 0, 1$, the magnetic field model is a conventional dipole model. When using magnetometers for attitude determination an onboard model of the field is required, and the choice of degree and order of the magnetic field depends on the desired accuracy needed; it is desirable to have a relatively good approximation of the field without requiring large calculating capabilities.

2) Magnetic control principles: Spacecraft with pure magnetic determination and control systems are typically equipped with orthogonally mounted magnetometers and magnetic torquers. The former are used for measurement of the magnetic field vectors, which forms the basis (often together with other types of measurements) for attitude determination. The latter are used for attitude control; being typically constructed as copper windings, they are able to generate a magnetic moment when a current is sent through the coil, and this magnetic moment subsequently reacts with the Earth magnetic field to provide a rotational torque. With this approach, the total torque generated on the spacecraft may be expressed in $\mathcal{F}^b$ as [32]

$$\boldsymbol{\tau} = \mathbf{S}(\mathbf{m}^b)\mathbf{b}^b\,, \tag{9}$$

where $\mathbf{m}^b$ is the magnetic dipole moment and $\mathbf{b}^b$ is the local geomagnetic field vector. As is obvious from (9), the available control torque approaches zero when the dipole moment vector and the local field vector align, and is lost completely when they are parallel. Such properties of controllability in magnetically actuated spacecraft is a very important topic, and has been thoroughly presented in [13]. Without going into detail of the latter reference, we suffice to say that definitions of strong accessibility and controllability of general time-varying systems are extended to the case of systems evolving on the rotational sphere in a time-varying magnetic field. However, for substantiation of our main result, we introduce to this end the following definition.

Definition 1 (Sufficiently accessible): The system in (5)-(6) is said to be sufficiently accessible on $\mathcal{M} = S^3 \times \mathbb{R}^3$ if there exists a constant $\delta > 0$ such that

$$\|\mathbf{S}^\top\left(\mathbf{b}^b\left(t\right)\right)\mathbf{S}\left(\mathbf{b}^b\left(t\right)\right)\| \geq \delta \quad \forall\ t \geq t_0\,. \tag{10}$$

We also note that $\mathbf{b}^b = \mathbf{R}_i^b \mathbf{b}^i$ and hence obtain

$$\dot{\mathbf{b}}^b = -\mathbf{S}\left(\boldsymbol{\omega}\right)\mathbf{b}^b + \mathbf{R}_i^b \dot{\mathbf{b}}^i\,. \tag{11}$$

IV. MAIN RESULT

A. Problem Definition

The problem is to design a control solution using magnetometer rate feedback such that the system is able to track a desired attitude trajectory $\mathbf{q}_d$, where $\dot{\mathbf{q}}_d = \mathbf{T}\left(\mathbf{q}_d\right)\boldsymbol{\omega}_d$ with $\boldsymbol{\omega}_d$ as the desired angular velocity. Using the quaternion product (3), we obtain the attitude error quaternion as $\tilde{\mathbf{q}} = \mathbf{q}_d^{-1} \otimes \mathbf{q}$, and in accordance with (5) we also have $\dot{\tilde{\mathbf{q}}} = \mathbf{T}\left(\tilde{\mathbf{q}}\right)\tilde{\boldsymbol{\omega}}$ with $\tilde{\boldsymbol{\omega}} = \boldsymbol{\omega} - \boldsymbol{\omega}_d$.

To uniquely define the attitude error, we now note that due to a redundancy in the quaternion representation, $\tilde{\mathbf{q}}$ and $-\tilde{\mathbf{q}}$ represent the same physical orientation, however one is rotated 2π relative to the other about an arbitrary axis. This phenomenon is physically explainable by the fact that when using quaternions, each orientation may be reached in two ways; *i.e.* we may rotate either clockwise or anti-clockwise about the rotation axis to reach the desired orientation. Accordingly, there exist two equilibrium points in the closed-loop system, namely $\tilde{\mathbf{q}}_+ = \left[1, \mathbf{0}^\top\right]^\top$ and $\tilde{\mathbf{q}}_- = \left[-1, \mathbf{0}^\top\right]^\top$. For optimality in terms of rotation length, one should choose the equilibrium point offering the shortest rotation – *cf.* [33].

For the sake of simplicity in our presentation, we choose the positive equilibrium point as our desired one [1]. Based on this choice, we define the attitude error

$$\mathbf{e}_q := \left[1 - \tilde{\eta},\ \tilde{\boldsymbol{\epsilon}}\right] \tag{12}$$

together with the angular velocity error

$$\mathbf{e}_\omega := \tilde{\boldsymbol{\omega}} = \boldsymbol{\omega} - \boldsymbol{\omega}_d \tag{13}$$

and the problem is thus to achieve $\lim_{t\to\infty}\left[\mathbf{e}_q,\ \mathbf{e}_\omega\right] \to \mathbf{0}$. In accordance with general kinematic relations we have

$$\dot{\mathbf{e}}_q = \mathbf{T}_e\left(\mathbf{e}_q\right)\mathbf{e}_\omega \tag{14}$$

[1]Note however that the negative equilibrium point still persists in our closed loop, and we are therefore not able to claim any global stability properties. In addition, the term global in general refers to the whole state space $\mathbb{R}^n$ (*cf.* [34]), while our system evolves on $\mathcal{M} = S^3 \times \mathbb{R}^3$.

with

$$\mathbf{T}_e\left(\mathbf{e}_q\right) = \frac{1}{2}\begin{bmatrix} \tilde{\boldsymbol{\epsilon}}^\top \\ \tilde{\eta}\mathbf{I} + \mathbf{S}\left(\tilde{\boldsymbol{\epsilon}}\right) \end{bmatrix}. \tag{15}$$

Moreover, the error dynamics are obtained from (13) and (6) as

$$\mathbf{J}\dot{\mathbf{e}}_\omega = \boldsymbol{\tau} - \mathbf{S}\left(\boldsymbol{\omega}\right)\mathbf{J}\boldsymbol{\omega} - \mathbf{J}\dot{\boldsymbol{\omega}}_d\,. \tag{16}$$

Further, we note that $4\mathbf{T}_e^\top\mathbf{T}_e = \mathbf{I}$, which can be shown by direct calculation and using $\mathbf{S}^\top(\tilde{\boldsymbol{\epsilon}}) = -\mathbf{S}\left(\tilde{\boldsymbol{\epsilon}}\right)$, $\mathbf{S}^\top\left(\tilde{\boldsymbol{\epsilon}}\right)\mathbf{S}\left(\tilde{\boldsymbol{\epsilon}}\right) = \tilde{\boldsymbol{\epsilon}}^\top\tilde{\boldsymbol{\epsilon}}\mathbf{I} - \tilde{\boldsymbol{\epsilon}}\tilde{\boldsymbol{\epsilon}}^\top$ and (2). We also note that $2\mathbf{T}_e^\top\left(\mathbf{e}_q\right)\mathbf{e}_q = \tilde{\boldsymbol{\epsilon}}$, and from differentiation of this result we obtain

$$\dot{\mathbf{T}}_e^\top\left(\mathbf{e}_q\right)\mathbf{e}_q = \frac{1}{2}\dot{\tilde{\boldsymbol{\epsilon}}} - \mathbf{T}_e^\top\left(\mathbf{e}_q\right)\dot{\mathbf{e}}_q \tag{17}$$

$$= \frac{1}{4}\left[\tilde{\eta}\mathbf{I} + \mathbf{S}\left(\tilde{\boldsymbol{\epsilon}}\right)\right]\mathbf{e}_\omega - \frac{1}{4}\mathbf{e}_\omega \tag{18}$$

$$= \mathbf{G}\mathbf{e}_\omega \tag{19}$$

with

$$\mathbf{G} = \frac{1}{4}\left[\tilde{\eta}\mathbf{I} + \mathbf{S}\left(\tilde{\boldsymbol{\epsilon}}\right) - \mathbf{I}\right]. \tag{20}$$

To fit with the choice of equilibrium point, it is also assumed that the scalar parameter of the quaternion is always positive, such that

$$\tilde{\eta}\left(t\right) > 0\,, \qquad \forall\ t \geq t_0\,. \tag{21}$$

B. Control solution

Having appropriately defined our control problem, we are now ready to state our main results, and the idea is the following. For small spacecraft, light and small is better in terms of instrumentation. However, sensors are necessary to provide continuous attitude determination, and combinations of solar sensors and magnetometers are common choices. Magnetometers are also commonly used in the initial detumbling phase when the angular velocity is too high to achieve attitude determination; by using a detumbling controller based on magnetometer rate feedback the spacecraft angular velocity may be reduced sufficiently to enter the operational phase. One of the classical approaches to magnetic control, and detumbling in particular, is the b-dot controller in [3], which has later been reproduced in various ways (*cf.* [8]).

The idea for our control solution is to combine a b-dot algorithm with a passivity-based control law, thus constructing a control law without angular velocity measurements in the common sense (*i.e.* by using gyroscopes, observers and/or lead filters). The solution is based on the standard PD+ controller from [26], but where the derivative term is replaced by magnetometer rate feedback. Moreover, some additional terms have been included to compensate for magnetometer coupling terms. This rationale may thus be summarized as the following proposition:

Proposition 2: Assume that (2) and (21) hold, and that the desired attitude $\mathbf{q}_d\left(t\right)$, desired angular velocity $\boldsymbol{\omega}_d\left(t\right)$ and desired angular acceleration $\dot{\boldsymbol{\omega}}_d\left(t\right)$ are all bounded functions.

Moreover, assume that the system dynamics (14)-(16), in closed loop with the control law

$$\begin{aligned}\boldsymbol{\tau} = &- k_p \mathbf{T}_e^\top \mathbf{e}_q - k_b \mathbf{S}\left(\dot{\mathbf{b}}^b\right)\mathbf{b}^b + \mathbf{J}\dot{\boldsymbol{\omega}}_d + \mathbf{S}\left(\boldsymbol{\omega}_d\right)\mathbf{J}\boldsymbol{\omega}_d \\ &+ k_b \mathbf{S}^\top\left(\mathbf{b}^b\right)\left[\mathbf{S}\left(\mathbf{b}^b\right)\boldsymbol{\omega}_d + \mathbf{R}_i^b \dot{\mathbf{b}}^i\right]\end{aligned} \tag{22}$$

with k_p and k_b as positive tuning parameters, is sufficiently accessible according to Definition 1. Then the equilibrium point $[\mathbf{e}_q, \mathbf{e}_\omega] = \mathbf{0}$ of the closed-loop system is uniformly asymptotically stable (UAS).

Remark 3: Note that in Proposition 2 it is assumed that the closed-loop system is sufficiently accessible according to Definition 1, which puts a restriction on the available orientations of the spacecraft relative to the surrounding magnetic field. In particular, we assume that $\|\mathbf{S}^\top\left(\mathbf{b}^b\right)\mathbf{S}\left(\mathbf{b}^b\right)\| \geq \delta > 0$; however, since $\mathbf{S}\left(\mathbf{b}^b\right)$ is a skew-symmetric matrix, the smallest eigenvalues of $\mathbf{S}^\top\left(\mathbf{b}^b\right)\mathbf{S}\left(\mathbf{b}^b\right)$ is $\lambda_1 = 0$, while the other two eigenvalues are given as $\lambda_2 = \lambda_3 = \left(\mathbf{b}^b\right)^\top \mathbf{b}^b$. Hence, the assumption of sufficient accessibility will not hold for all orientations as a result of the nature of the magnetic field. However, if such a situation occurs, the system will lose its damping, and it is reasonable to assume that it will thereby drift into an orientation where the closed-loop system will regain sufficient accessibility.

Remark 4: The control law (22) assumes the knowledge of magnetometer rates $\dot{\mathbf{b}}^b$ and $\dot{\mathbf{b}}^i$. The magnetic field vector is measured in $\mathcal{F}^b$, and although the body frame magnetometer rate $\dot{\mathbf{b}}^b$ may be extracted through a differentiation filter, the inertial magnetometer rate $\dot{\mathbf{b}}^i$ is not as easily calculated. One approach is to use (11), such that

$$\dot{\mathbf{b}}^i = \mathbf{R}_b^i\left(\dot{\mathbf{b}}^b + \mathbf{S}\left(\boldsymbol{\omega}\right)\mathbf{b}^b\right) \tag{23}$$

however this requires knowledge of the actual angular rate $\boldsymbol{\omega}$. Similarly, the control law (22) assumes the knowledge of desired angular rate $\boldsymbol{\omega}_d$ and its derivative $\dot{\boldsymbol{\omega}}_d$, both represented in $\mathcal{F}^b$. The desired angular velocity is typically given in $\mathcal{F}^i$, and hence the rate is easily extracted through the coordinate transformation $\boldsymbol{\omega}_d = \mathbf{R}_i^b \boldsymbol{\omega}_d^i$. However, the derivative must be extracted from the relation

$$\dot{\boldsymbol{\omega}}_d = -\mathbf{S}\left(\boldsymbol{\omega}\right)\boldsymbol{\omega}_d + \mathbf{R}_i^b \dot{\boldsymbol{\omega}}_d^i \tag{24}$$

and also this requiring knowledge of actual angular velocity. Both of the above cases can be approximated using modified relations (*cf.* [21]) where $\boldsymbol{\omega}$ is replaced with $\boldsymbol{\omega}_d$, such that

$$\hat{\dot{\mathbf{b}}}^i = \mathbf{R}_b^i\left(\dot{\mathbf{b}}^b + \mathbf{S}\left(\boldsymbol{\omega}_d\right)\mathbf{b}^b\right) \tag{25}$$

and

$$\hat{\dot{\boldsymbol{\omega}}}_d = -\mathbf{S}\left(\boldsymbol{\omega}_d\right)\boldsymbol{\omega}_d + \mathbf{R}_i^b \dot{\boldsymbol{\omega}}_d^i = \mathbf{R}_i^b \dot{\boldsymbol{\omega}}_d^i\,. \tag{26}$$

This will probably give some uncertainty in the initial transient, but will provide a good approximation close to the reference trajectory.

Remark 5: Also note that Proposition 2 is stated for the case when (21) holds, and with the positive equilibrium point as the chosen one; however, a similar argument may be stated for the negative equilibrium point, in the case when $\tilde{\eta}(t) < 0,\ \forall\, t \geq t_0$ (*cf.* [33]).

Proof: Inserting the control law (22) in (16) results in

$$\begin{aligned}\mathbf{J}\dot{\mathbf{e}}_\omega = &-k_p \mathbf{T}_e^\top \mathbf{e}_q - k_b \mathbf{S}\left(\dot{\mathbf{b}}^b\right)\mathbf{b}^b - \mathbf{S}\left(\boldsymbol{\omega}\right)\mathbf{J}\boldsymbol{\omega} \\ &+ \mathbf{S}\left(\boldsymbol{\omega}_d\right)\mathbf{J}\boldsymbol{\omega}_d + k_b \mathbf{S}^\top\left(\mathbf{b}^b\right)\left[\mathbf{S}\left(\mathbf{b}^b\right)\boldsymbol{\omega}_d + \mathbf{R}_i^b \dot{\mathbf{b}}^i\right]\end{aligned} \tag{27}$$

and using (11), together with the facts that for arbitrary vectors $\mathbf{u}$ and $\mathbf{v}$ we have $\mathbf{u}^\top \mathbf{S}\left(\mathbf{u}\right) = -\mathbf{S}(\mathbf{u})\mathbf{u} = \mathbf{0}$, $\mathbf{S}^\top\left(\mathbf{u}\right) = -\mathbf{S}\left(\mathbf{u}\right)$ and $\mathbf{S}\left(\mathbf{u}\right)\mathbf{v} = -\mathbf{S}\left(\mathbf{v}\right)\mathbf{u}$, we find that

$$\begin{aligned}\mathbf{J}\dot{\mathbf{e}}_\omega = &- k_p \mathbf{T}_e^\top \mathbf{e}_q - k_b \mathbf{S}^\top\left(\mathbf{b}^b\right)\mathbf{S}\left(\mathbf{b}^b\right)\mathbf{e}_\omega \\ &- \mathbf{S}\left(\boldsymbol{\omega}\right)\mathbf{J}\boldsymbol{\omega} + \mathbf{S}\left(\boldsymbol{\omega}_d\right)\mathbf{J}\boldsymbol{\omega}_d\end{aligned} \tag{28}$$

and the total closed-loop system is thus given by

$$\dot{\mathbf{e}}_q = \mathbf{T}_e \mathbf{e}_\omega \tag{29}$$

$$\begin{aligned}\mathbf{J}\dot{\mathbf{e}}_\omega = &- k_p \mathbf{T}_e^\top \mathbf{e}_q - k_b \mathbf{S}^\top\left(\mathbf{b}^b\right)\mathbf{S}\left(\mathbf{b}^b\right)\mathbf{e}_\omega \\ &- \mathbf{S}\left(\boldsymbol{\omega}\right)\mathbf{J}\boldsymbol{\omega} + \mathbf{S}\left(\boldsymbol{\omega}_d\right)\mathbf{J}\boldsymbol{\omega}_d\,.\end{aligned} \tag{30}$$

To prove Proposition 2, we define the state vector $\boldsymbol{\chi} = [\boldsymbol{\chi}_1, \boldsymbol{\chi}_2] = \left[\mathbf{e}_q^\top \mathbf{T}_e, \mathbf{e}_\omega\right]$, together with the Lyapunov function candidate

$$V\left(\boldsymbol{\chi}\right) = \frac{1}{2}\mathbf{e}_q^\top k_p \mathbf{e}_q + \frac{1}{2}\mathbf{e}_\omega^\top \mathbf{J}\mathbf{e}_\omega + \lambda \mathbf{e}_q^\top \mathbf{T}_e \mathbf{J}\mathbf{e}_\omega \tag{31}$$

with $\lambda > 0$ as a design variable. By using the property in (4) we obtain for the first term in (31) that

$$\begin{aligned}\frac{1}{2}\mathbf{e}_q^\top k_p \mathbf{e}_q =& \frac{1}{2}k_p\left(\left(1 - \tilde{\eta}\right)^2 + \tilde{\boldsymbol{\epsilon}}^\top \tilde{\boldsymbol{\epsilon}}\right) \\ &\leq k_p \tilde{\boldsymbol{\epsilon}}^\top \tilde{\boldsymbol{\epsilon}} = \mathbf{e}_q^\top \mathbf{T}_e k_p \mathbf{T}_e^\top \mathbf{e}_q\,.\end{aligned} \tag{32}$$

At the other end, we have that

$$\frac{1}{2}\mathbf{e}_q^\top k_p \mathbf{e}_q \geq \frac{1}{2}\mathbf{e}_q^\top \mathbf{T}_e k_p \mathbf{T}_e^\top \mathbf{e}_q\,. \tag{33}$$

Accordingly, we may write

$$V\left(\boldsymbol{\chi}\right) \leq \frac{1}{2}\boldsymbol{\chi}^\top \mathbf{P}\boldsymbol{\chi}, \qquad \mathbf{P} = \begin{bmatrix} k_p \mathbf{I} & \lambda \mathbf{J} \\ \lambda \mathbf{J} & \mathbf{J}\end{bmatrix} \tag{34}$$

and it follows that $V\left(\boldsymbol{\chi}\right)$ satisfies

$$\frac{1}{4}p_m\|\boldsymbol{\chi}\|^2 \leq V\left(\boldsymbol{\chi}\right) \leq \frac{1}{2}p_M\|\boldsymbol{\chi}\|^2 \tag{35}$$

with p_m and p_M as the smallest and largest eigenvalue of $\mathbf{P}$, respectively. Employing the Schur complement (*cf.* [35]), we find that the matrix $\mathbf{P}$ is positive for $k_p > 0$ and

$$\lambda^2 \leq \frac{2k_p j_m}{j_M^2}\,. \tag{36}$$

By taking the derivative of (31) along the system trajectories (29)-(30), and employing (13) and (17)-(19), we obtain

$$\begin{aligned}\dot{V} = &- \mathbf{e}_\omega^\top k_b \mathbf{S}^\top\left(\mathbf{b}^b\right)\mathbf{S}\left(\mathbf{b}^b\right)\mathbf{e}_\omega - \mathbf{e}_\omega^\top \mathbf{S}\left(\boldsymbol{\omega}_d\right)\mathbf{J}\mathbf{e}_\omega \\ &- \lambda \mathbf{e}_q^\top \mathbf{T}_e k_p \mathbf{T}_e^\top \mathbf{e}_q - \lambda \mathbf{e}_q^\top \mathbf{T}_e k_b \mathbf{S}^\top\left(\mathbf{b}^b\right)\mathbf{S}\left(\mathbf{b}^b\right)\mathbf{e}_\omega \\ &- \lambda \mathbf{e}_q^\top \mathbf{T}_e \mathbf{S}\left(\mathbf{e}_\omega\right)\mathbf{J}\mathbf{e}_\omega - \lambda \mathbf{e}_q^\top \mathbf{T}_e \mathbf{S}\left(\mathbf{e}_\omega\right)\mathbf{J}\boldsymbol{\omega}_d \\ &- \lambda \mathbf{e}_q^\top \mathbf{T}_e \mathbf{S}\left(\boldsymbol{\omega}_d\right)\mathbf{J}\mathbf{e}_\omega + \lambda \mathbf{e}_\omega^\top \mathbf{J}\mathbf{T}_e^\top \mathbf{T}_e \mathbf{e}_\omega + \lambda \mathbf{e}_\omega^\top \mathbf{J}\mathbf{G}\mathbf{e}_\omega\,.\end{aligned} \tag{37}$$

Rearranging terms and using (20) together with the facts that $4\mathbf{T}_e^\top \mathbf{T}_e = \mathbf{I}$ and $2\mathbf{T}_e^\top \mathbf{e}_q = \tilde{\boldsymbol{\epsilon}}$, we find that

$$\begin{aligned}\dot{V} = &-\lambda \mathbf{e}_q^\top \mathbf{T}_e k_p \mathbf{T}_e^\top \mathbf{e}_q - \mathbf{e}_\omega^\top \Big[k_b \mathbf{S}^\top(\mathbf{b}^b)\mathbf{S}(\mathbf{b}^b) + \mathbf{S}(\boldsymbol{\omega}_d)\mathbf{J} \\ &-\lambda\frac{1}{4}\mathbf{J}\left[\tilde{\eta}\mathbf{I} - \mathbf{S}(\tilde{\boldsymbol{\epsilon}})\right]\Big]\mathbf{e}_\omega - \mathbf{e}_q^\top \mathbf{T}_e \Big[\lambda k_b \mathbf{S}^\top(\mathbf{b}^b)\mathbf{S}(\mathbf{b}^b) \\ &-\lambda \mathbf{S}(\mathbf{J}\boldsymbol{\omega}_d) + \lambda \mathbf{S}(\boldsymbol{\omega}_d)\mathbf{J}\Big]\mathbf{e}_\omega . \end{aligned} \tag{38}$$

Accordingly, we obtain the Lyapunov function derivative

$$\dot{V}(\boldsymbol{\chi}) = -\boldsymbol{\chi}^\top \mathbf{Q}(\boldsymbol{\chi})\boldsymbol{\chi}, \quad \mathbf{Q}(\boldsymbol{\chi}) = [q_{ij}]\,, i,j = 1,2 \tag{39}$$

with

$$\begin{aligned} q_{11} &= \lambda k_p \mathbf{I} \\ q_{12} &= q_{12}^\top = \frac{\lambda}{2}\left(k_b \mathbf{S}^\top(\mathbf{b}^b)\mathbf{S}(\mathbf{b}^b) - \mathbf{S}(\mathbf{J}\boldsymbol{\omega}_d) + \mathbf{S}(\boldsymbol{\omega}_d)\mathbf{J}\right) \\ q_{22} &= k_b \mathbf{S}^\top(\mathbf{b}^b)\mathbf{S}(\mathbf{b}^b) + \mathbf{S}(\boldsymbol{\omega}_d)\mathbf{J} - \lambda\frac{1}{4}\mathbf{J}\left[\tilde{\eta}\mathbf{I} - \mathbf{S}(\tilde{\boldsymbol{\epsilon}})\right] . \end{aligned}$$

To verify negative definiteness of the Lyapunov function derivative, we again employ Schur's complement to obtain that the matrix $\mathbf{Q}$ is positive definite if and only if both q_{11} and $q_{22} - q_{21}q_{11}^{-1}q_{12}$ are positive definite. We first impose an upper bound on the desired angular velocity, such that $\|\boldsymbol{\omega}_d\| \leq \beta_d$, and also an upper bound on the magnetic field vector $\mathbf{b}^b$, such that $\|\mathbf{S}^\top(\mathbf{b}^b)\mathbf{S}(\mathbf{b}^b)\| \leq \beta_b$. The latter is a reasonable assumption, based on the physical nature of the magnetic field. We also recollect the assumption of sufficient accessibility, such that $\|\mathbf{S}^\top(\mathbf{b}^b)\mathbf{S}(\mathbf{b}^b)\| \geq \delta$. Hence, since $k_p > 0$ by definition, we find by taking the norm of the submatrices in $\mathbf{Q}$ that the latter is positive definite if

$$\lambda \leq \frac{2k_p(k_b\delta - j_M\beta_d)}{(k_b\beta_b + 2j_M\beta_d)^2 + j_M} \tag{40}$$

and to ensure $\lambda > 0$ we impose the restriction

$$k_b > \frac{j_M\beta_d}{\delta} . \tag{41}$$

Hence, if the controller gain k_b is chosen according to (41), and the design constant λ is chosen according to (36) and (40), we find that for all admissible $\boldsymbol{\chi}$, $V(\boldsymbol{\chi})$ is positive definite and $\dot{V}(\boldsymbol{\chi})$ is negative definite, and in light of the bound (35) it follows from standard Lyapunov arguments that the equilibrium point $[\mathbf{e}_q, \mathbf{e}_\omega] = \mathbf{0}$ of the closed-loop system is UAS. ■

Remark 6: Note that for both the special cases of setpoint regulation such that $\boldsymbol{\omega}_d = \mathbf{0}$, and cubic spacecraft such that the matrix of inertial moments is given by $\mathbf{J} = j\mathbf{I}$, the gain conditions are relaxed to the trivial $k_p > 0$ and $k_b > 0$. The latter case follows from the loss of the term $\mathbf{S}(\boldsymbol{\omega}_d)\mathbf{J}$ in q_{22}, since this term becomes skew-symmetric when $\mathbf{J} = j\mathbf{I}$.

V. SIMULATIONS

To visualize the performance of the control solution, we include simulations results of the system (14)-(16) in closed loop with the control law (22). The spacecraft has moments of inertia given by $\mathbf{J} = \mathrm{diag}\ \{0.017,\ 0.012,\ 0.015\}\ \mathrm{kgm}^2$, and is set to orbit the Earth in a slightly elliptic orbit with apogee altitude of 700 km and perigee altitude of 600 km, with inclination of 75 degrees. This represents an almost polar orbit with starting position for the spacecraft over the equator. For simplicity, the magnetic field of the Earth is simulated with a simple dipole model.

The initial conditions of the spacecraft are standstill with an attitude of $\boldsymbol{\Theta}(t_0) = [-45\ 50\ 30]^\top$ degrees, corresponding approximately to $\mathbf{q}(t_0) = [0.77\ -0.44\ 0.29\ 0.37]^\top$, and the spacecraft is further commanded to track a nadir-pointing trajectory. With this simulation setup, we find upper bounds for the desired angular velocity and magnetic field vector as $\beta_d = 1.1 \cdot 10^{-3}$ and $\beta_b = 4.5 \cdot 10^{-5}$, respectively, and the bound for sufficient accessibility is set to $\delta = 2 \cdot 10^{-5}$. Based on these bounds, we satisfy the gain constraint in (41) with $k_p = 5 \cdot 10^{-7}$ and $k_b = 5 \cdot 10^4$. With these gains, the resulting bound given by (36) and (40) is $\lambda \leq 7 \cdot 10^{-11}$.

A simulation over 12000 seconds (approximately 2 orbits) was performed, and the resulting attitude and angular velocity errors are shown in the two topmost plots in Fig. 1. The figure shows that the control law successfully stabilizes the attitude and angular velocity, and enables the spacecraft to track the desired trajectory. The bottommost plot in Fig. 1 shows the magnitude of the damping term, and it is seen that this corresponds with the location of the spacecraft such that its magnitude is smaller at the poles than at the equator. It is also seen that the asymptotic convergence is faster at the location where the damping term is larger. This effect is also visible in Fig. 2, which shows that the Lyapunov function is

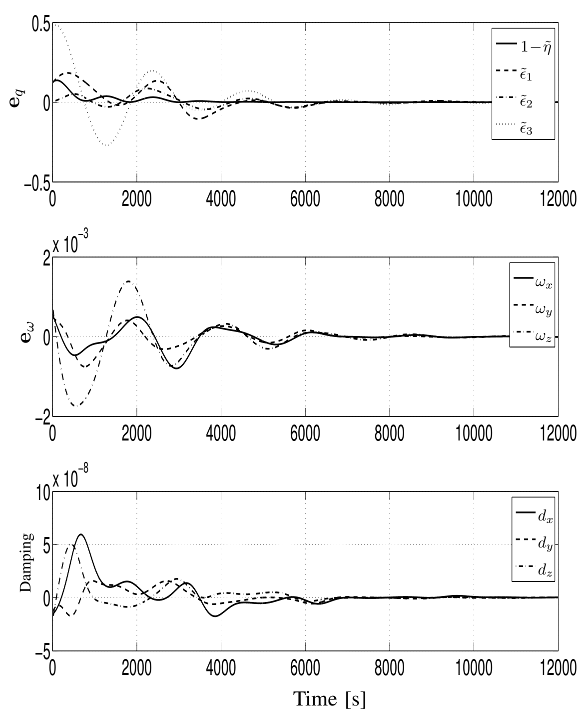

Fig. 1. Result of simulation over approximately two orbits. The plot shows attitude error, angular velocity error and magnitude of damping term.

constantly decaying, however that the convergence rate is reduced when the spacecraft is close to the poles.

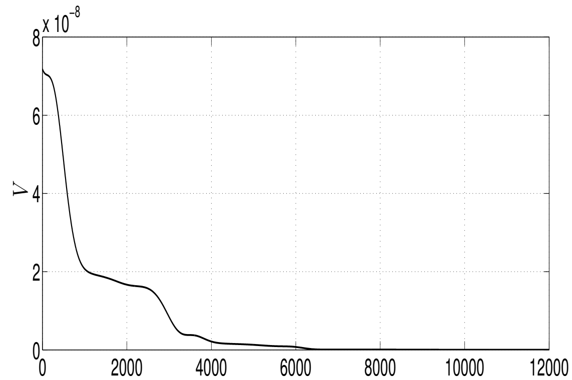

Fig. 2. Evolution of the chosen Lyapunov function during the simulation.

VI. CONCLUSIONS

We have presented a solution to spacecraft attitude tracking control utilizing a passivity-based PD+ control solution incorporating magnetometer rate feedback to obtain damping effect instead of classical sensors for angular velocity. The chosen equilibrium point of the closed-loop system has been proved to be uniformly asymptotically stable (UAS) under some mild gain conditions, and the performance of the tracking controller has been visualized through simulations.

REFERENCES

[1] J. R. Wertz, Ed., *Spacecraft Attitude Determination and Control*, ser. Astrophysics and Space Science Library. London, UK: Kluwer Academic Publishers, 1978, ISBN: 978-9027712042.

[2] E. Silani and M. Lovera, "Magnetic spacecraft attitude control: a survey and some new results," *Control Engineering Practice*, vol. 13, no. 3, pp. 357–371, 2005.

[3] A. Stickler and K. T. Alfriend, "An elementary magnetic attitude control system," *Journal of Spacecraft and Rockets*, vol. 13, no. 5, pp. 282–287, 1976.

[4] F. Martel, P. Pal, and M. Psiaki, "Active magnetic control system for gravity gradient stabilized spacecraft," in *Proceedings of the 2nd annual AIAA/USU Conference on Small Satellites*, Logan, Utah, 1988.

[5] R. Wiśniewski, "Satellite attitude control using only electromagnetic actuation," Ph.D. dissertation, Department of Control Engineering, Aalborg University, Aalborg, Denmark, 1996.

[6] R. Wisniewski and M. Blanke, "Fully magnetic attitude control for spacecraft subject to gravity gradient," *Automatica*, vol. 35, no. 7, pp. 1201–1214, 1999.

[7] R. Wisniewski, "Linear time-varying approach to satellite attitude control using only electromagnetic actuation," *Journal of Guidance, Control and Dynamics*, vol. 23, no. 4, pp. 640–646, 2000.

[8] J. Gravdahl, E. Eide, A. Skavhaug, K. M. Fauske, K. Svartveit, and F. M. Indergaard, "Three axis attitude determination and control system for a picosatellite: Design and implementation," in *Proceedings of the 54th International Astronautical Congress*, Bremen, Germany, 2003.

[9] M. Lovera and A. Astolfi, "Spacecraft attitude control using magnetic actuators," *Automatica*, vol. 40, no. 8, pp. 1405–1414, 2004.

[10] M. Grassi, "Attitude determination and control for a small remote sensing satellite," *Acta Astronautica*, vol. 40, no. 9, pp. 675–681, 1997.

[11] D. Lebedev and A. Tkachenko, "Magnetic attitude control system for low-earth orbit satellites," *Multibody System Dynamics*, vol. 6, no. 1, pp. 29–37, 2001.

[12] V. A. Bushenkov, M. Y. Ovchinnikov, and G. V. Smirnov, "Attitude stabilization of a satellite by magnetic coils," *Acta Astronautica*, vol. 50, no. 12, pp. 721–728, 2002.

[13] S. P. Bhat, "Controllability of nonlinear time-varying systems: Applications to spacecraft attitude control using magnetic actuation," *IEEE Transactions on Automatic Control*, vol. 50, no. 11, pp. 1725–1735, 2005.

[14] J. T.-Y. Wen and K. Kreutz-Delgado, "The attitude control problem," *IEEE Transactions on Automatic Control*, vol. 36, no. 10, pp. 1148–1162, 1991.

[15] J.-M. Godhavn and O. Egeland, "Attitude control of an underactuated satellite," in *Proceedings of the 34th IEEE Conference on Decision and Control*, New Orleans, LA, 1995.

[16] M. M. Quottrup, J. Krogh-Sørensen, and R. Wiśniewski, "Passivity based nonlinear attitude control of the Rømer satellite," in *Proceedings of the 15th IFAC Symposium on Automatic Control in Aerospace*, Bologna, Italy, 2001.

[17] R. Schlanbusch, K. Reiten, R. Kristiansen, and P. J. Nicklasson, "Passivity-based attitude control of the SSETI ESMO satellite," in *Proceedings of the 9th International Conference on Exploration and Utilisation of the Moon*, Sorento, Italy, 2007.

[18] F. Caccavale, C. Natale, and L. Villani, "Output feedback control of mechanical systems with application to spacecraft and robots," *AIAA Journal of Guidance, Control and Dynamics*, vol. 26, no. 2, pp. 273–282, 2003.

[19] D. Seo and M. R. Akella, "Separation property for the rigid-body attitude tracking control problem," *AIAA Journal of Guidance, Control and Dynamics*, vol. 30, no. 6, pp. 1569–1576, 2007.

[20] F. Lizarralde and J. T. Wen, "Attitude control without angular velocity measurement: a passivity approach," *IEEE Transactions on Automatic Control*, vol. 41, no. 3, pp. 468–472, 1996.

[21] F. Caccavale and L. Villani, "Output feedback control for attitude tracking," *Systems & Control Letters*, vol. 38, no. 2, pp. 91–98, 1999.

[22] B. Costic, D. Dawson, M. de Queiroz, and V. Kapila, "A quaternion-based adaptive attitude tracking controller without velocity measurements," in *Proceedings of the IEEE Conference on Decision and Control*, Sydney, Australia, 2000.

[23] K. Subbarao and M. R. Akella, "Differentiator-free nonlinear proportional-integral controllers for rigid-body attitude stabilization," *AIAA Journal of Guidance, Control and Dynamics*, vol. 27, no. 6, pp. 1092–1096, 2004.

[24] M. R. Akella, A. Valdivia, and G. R. Kotamraju, "Velocity-free attitude controllers subject to actuator magnitude and rate saturations," *AIAA Journal of Guidance, Control and Dynamics*, vol. 28, no. 4, pp. 659–666, 2005.

[25] P. Singla, K. Subbarao, and J. L. Junkins, "Adaptive output feedback control for spacecraft rendezvous and docking under measurement uncertainty," *AIAA Journal of Guidance, Control and Dynamics*, vol. 29, no. 4, pp. 892–902, 2006.

[26] B. Paden and R. Panja, "Globally asymptotically stable 'PD+' controller for robot manipulators," *International Journal of Control*, vol. 47, no. 6, pp. 1697–1712, 1988.

[27] R. Ortega, A. Loría, P. J. Nicklasson, and H. Sira-Ramírez, *Passivity-based Control of Euler-Lagrange Systems: Mechanical, Electrical and Electromechanical Applications*, ser. Communications and Control Engineering. London, UK: Springer-Verlag, 1998.

[28] C. J. Damaren, "Hybrid magnetic attitude control gain selection," in *Proceedings of the IMechE, Part G: Journal of Aerospace Engineering*, vol. 223, no. G8, 2009, pp. 1041–1048.

[29] O. Egeland and J. T. Gravdahl, *Modeling and Simulation for Automatic Control*. Trondheim, Norway: Marine Cybernetics, 2002.

[30] M. D. Shuster and S. D. Oh, "Three-axis attitude determination from vector observations," *Journal of Guidance and Control*, vol. 4, no. 1, pp. 70–77, 1981.

[31] W. H. Campbell, *Introduction to geomagnetic fields*. Canbridge, UK: Cambridge University Press, 1997.

[32] S. V. Marshall and G. G. Skitek, *Electromagnetic Concepts and Applications*. New Jersey, USA: Prentice-Hall International Inc., 1989.

[33] R. Kristiansen, A. Loría, A. Chaillet, and P. J. Nicklasson, "Spacecraft relative rotation tracking without angular velocity measurements," *Automatica*, vol. 45, no. 3, pp. 750–756, 2009.

[34] W. Hahn, *Stability of Motion*. Berlin, Germany: Springer-Verlag, 1967.

[35] R. A. Horn and C. R. Johnson, *Matrix analysis*. Cambridge University Press, 1999.